Available online at www.sciencedirect.com
SCIENCE DIRECT
Journal of Magnetic Resonance 179 (2006) 250–262
JMR Journal of Magnetic Resonance
www.elsevier.com/locate/jmr

Field-dependent nuclear relaxation of spins 1/2 induced by dipole–dipole couplings to quadrupole spins: LaF_3 crystals as an example

Danuta Kruk [a,b,*], Oliver Lips [a]

[a] Institut für Festkörperphysik, TU Darmstadt, Hochschulstr. 6, 64289 Darmstadt, Germany
[b] Institute of Physics, Jagiellonian University, Reymonta 4, 30-059 Krakow, Poland

Received 15 September 2005; revised 15 December 2005
Available online 19 January 2006

Abstract

A general theory of spin–lattice nuclear relaxation of spins $I = 1/2$ caused by dipole–dipole couplings to quadrupole spins $S \geqslant 1$, characterized by a non-zero averaged (static) quadrupole coupling, is presented. In multispin systems containing quadrupolar and dipolar nuclei, transitions of spins 1/2 leading to their relaxation are associated through dipole–dipole couplings with certain transitions of quadrupole spins. The averaged quadrupole coupling attributes to the energy level structure of the quadrupole spin and influences in this manner relaxation processes of the spin 1/2. Typically, quadrupole spins exhibit also a complex multiexponential relaxation sensed by the dipolar spin as an additional modulation of the mutual dipole–dipole coupling. The proposed model includes both effects and is valid for an arbitrary magnetic field and an arbitrary quadrupole spin quantum number. The theory is applied to interpret fluorine relaxation profiles in LaF_3 ionic crystals. The obtained results are compared with predictions of the 'classical' Solomon relaxation theory.

Keywords: Nuclear relaxation; Quadrupole spins; Dipolar spins; Solid state; Ion dynamics

1. Introduction

Field-dependent relaxation studies can be an important source of information on dynamic properties of a system, provided that an adequate theoretical model is available. Fast development of field cycling techniques gives the possibility to perform relaxation experiments in a wide range of magnetic fields for a variety of multispin systems. In this context it is of primary importance to provide a reasonable theoretical tool for modeling and interpreting observed field dependencies of relaxation processes. The applicability of the 'classical' Solomon [1] and Solomon–Bloemberger–Morgan (SBM) descriptions [2–4] is strongly limited. The formulas are a special case of the general Redfield relaxation theory [5–7], based on a perturbation approach. The perturbation treatment assumes that a total spin Hamiltonian can be divided into two parts: the main, unperturbed part, which determines the energy level structure of the system, and the perturbing, time-dependent part with zero average, which causes transitions between the energy levels. The Solomon approach as well as its extension, including relaxation processes of the spin S (the SBM theory), have been developed under the assumption that Zeeman interactions are dominant for both spins relaxing through their mutual dipole–dipole coupling. This treatment breaks down for systems containing quadrupole spins, which exhibit a non-zero static quadrupole coupling. It can neither be applied to the quadrupole spin, $S \geqslant 1$, nor the dipolar spin, $I = 1/2$, coupled to the quadrupole one. The energy level structure of the quadrupole, high spin is determined by a superposition of a static quadrupole interaction and a Zeeman coupling, and depends on the orientation of the electric field gradient tensor at the position of the spin, with respect to the direction of the applied external

* Corresponding author. Fax: +49 6151 162833.
E-mail address: Danuta.Kruk@physik.tu-darmstadt.de (D. Kruk).

1090-7807/$ - see front matter © 2005 Elsevier Inc. All rights reserved.
doi:10.1016/j.jmr.2005.12.009

magnetic field. Only in the high field limit, when the Zeeman coupling is much stronger than the quadrupole interaction the high spin is quantized in the laboratory frame. The energy level structure of the quadrupole spin S, dominated at low magnetic fields by the static quadrupole interaction, as well as its complex dynamics resulting from this quantization, become relevant for relaxation processes of the dipolar spin I, when there is an I–S coupling.

In this paper, we elucidate effects of the quadrupolar coupling affecting relaxation dynamics of spins 1/2 via the mutual, dipolar spin-quadrupole–spin dipole–dipole interactions.

In multispin systems containing quadrupolar and dipolar nuclei, transitions of the spin 1/2 leading to its relaxation are associated through the dipole–dipole coupling to certain transitions of the quadrupole spin. Since dipolar interactions involve two spins, the static quadrupole coupling influences magnetic field dependencies of the dipolar relaxation of the spin I, by affecting the frequencies of the combined I–S transitions. In addition, the high spin nuclei can provide through their own relaxation mechanism a source of relaxation for dipolar nuclei. From the perspective of the spin 1/2 nucleus the relaxation processes of the quadrupole nucleus contributes to time fluctuations of the dipole–dipole coupling in a manner similar to other stochastic processes like for example jump diffusion. However, the quadrupole high-spin nuclei exhibit complex, multiexponential relaxation. Under certain motional conditions, discussed in the paper, well defined relaxation rates can be assigned to individual coherences associated with transitions of the quadrupole spin. Since the dipolar spin senses the various quadrupole relaxation rates corresponding to particular quadrupole spin modes and coherences, fluctuations of the mutual dipole–dipole coupling cannot be described any longer by one characteristic time constant. One needs to consider a set of correlation times containing the quadrupole relaxation contributions to the modulations of the dipole–dipole axis. It should be emphasized that magnetic field dependencies of the quadrupole relaxation rates are also affected by the static quadrupole coupling. If other dynamic processes affecting the dipole–dipole coupling (like for example jump diffusion) are on a rapid time scale relative to the quadrupole relaxation, the spread of the dipolar correlation times around the main value corresponding to the fastest motional process, becomes negligible. However, even in this motional limit, relaxation of the dipolar spin is affected by the static part of the quadrupole coupling attributing to the energy level structure of the quadrupole spin and influencing in this manner the dynamic of the spin 1/2. It is important to point out that our approach has also some limitations. We assume that the dipolar as well as quadrupole spins fulfill the conditions of the Redfield theory [5–7]; otherwise one could not explicitly define time-independent relaxation rates. The second limitation concerns the averaged (static) quadrupole coupling. All considerations presented here are dedicated to systems containing quadrupole spins, which exhibit a non-zero averaged quadrupole coupling attributing to their energy level structure and influencing relaxation processes of spins 1/2. It means, that we consider systems where eventual fluctuations (caused for example by a rotational motion) of the averaged quadrupole coupling relative to the laboratory frame are much slower than the relaxation of the quadrupole spin. The averaged quadrupole coupling is sensed by the quadrupole spin as a static interaction contributing to its energy level structure only under this motional condition. Thus, our model is dedicated mainly to solid state systems, where this condition is usually fulfilled. In general, depending on the strength of the averaged quadrupole coupling and the time scale of its fluctuation relative to the laboratory frame, the averaged quadrupole interaction can be sensed by the quadrupole spin as a main, static interaction, as a relaxation mechanism, or even it can bring the quadrupole spin outside validity regimes of the Redfield relaxation theory. This problem has been discussed in detail in the context of electron spin relaxation and a static zero field splitting in [8].

Nuclear relaxation of a spin 1/2 originating from a dipole–dipole coupling to another spin with a non-Zeeman energy level structure and its own (unrelated to any interactions with the spin 1/2) relaxation mechanism can be considered in a much more general context. A good example is the paramagnetic relaxation enhancement of a nuclear spin 1/2 (for example water protons) caused by its dipole–dipole coupling to an electron spin with energy levels resulting from a superposition of the electron Zeeman interaction and the zero field splitting and relaxing through time fluctuations of the zero field splitting tensor [9–12]. Since the quadrupole coupling as well as the zero field splitting are one-spin interactions expressed in terms of second-rank tensor operators, there are deep analogies between the two systems of interacting spins. We formulate in this paper, following the line of analogies between quadrupole and electron spin dynamics, a general description of spin–lattice relaxation of a dipolar spin 1/2 induced by its coupling to an ensemble of quadrupole spins, valid for an arbitrary magnetic field and arbitrary quadrupole spin quantum number. Our approach includes the effects of the static quadrupole coupling as well as the multiexponential quadrupole relaxation. We provide in this way a tool appropriate for an analysis of field-dependent relaxation studies for a variety of solid state systems containing dipolar as well as quadrupole spins with mutual dipole–dipole couplings. Our description can be treated as a 'quadrupole' counterpart of the paramagnetic relaxation enhancement theory [9,11,12] dedicated to solid-state systems.

We discuss the theoretical model in a close relation to fluorine spin–lattice relaxation in LaF_3 crystals, treating them as an example of systems under interest.

Section 2 contains a description of spin interactions and motional processes within the LaF_3 lattice relevant for the fluorine spin relaxation. Section 3 presents a general theory of spin–lattice relaxation of spins 1/2 induced by couplings to quadrupole spins, which is adapted in Section 4 to the

exemplary case of field-dependent fluorine spin relaxation in the LaF_3 crystal lattice. Section 5 contains examples of the fluorine relaxation profiles analyzed within the proposed theory and also illustrative comparisons of the present treatment with the classical Solomon approach [1]. Concluding remarks are covered in Section 6.

2. Mechanisms of fluorine spin relaxation in LaF_3 crystals

Our considerations begin with a discussion of mechanisms of fluorine spin relaxation in LaF_3 crystals. We shall point out the necessity to formulate a proper description of relaxation processes of the fluorine spins caused by their dipole–dipole couplings to the quadrupole, lanthanum spins.

The crystal LaF_3 has the tysonite structure ($P\bar{3}c1$), in which the fluorine ions occupy three distinct positions: F_1, F_2 and F_3, in the ratio 12:4:2 [13]. The sites F_2 and F_3 are structurally almost equivalent and therefore they can be treated as one in studies of fluorine relaxation processes [14]. The structure of LaF_3 is illustrated in Fig. 1, where views along and perpendicular to the c-axis are shown. We shall denote from now the two distinct sublattices F_1 and F_2–F_3 as F_A and F_B, respectively. Fluorine spins belonging to each of these sublattices are coupled by dipole–dipole interactions to fluorine spins from the same sublattice as well as to those from the second one, and they are also coupled to the lanthanum spins.

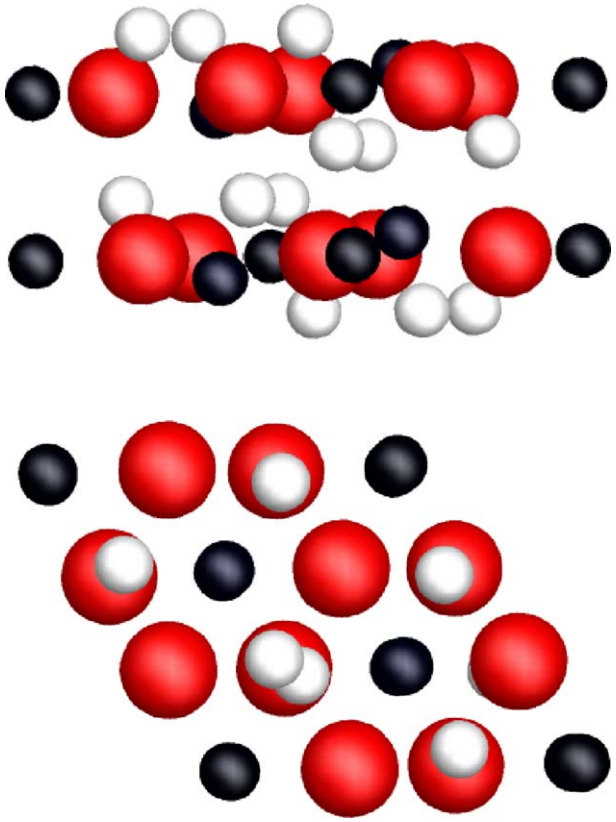

Fig. 1. Unit cell of LaF_3. The upper part shows a view perpendicular to the c-axis, the lower part a view along the c-axis. The lanthanum ions are represented by the large spheres, the F_1-ions are shown as light spheres, the F_2 and F_3 ions as dark spheres.

The I_i–P dipole–dipole coupling between the fluorine spin I_i and the spin P (where P denotes other fluorine spin I_j or a lanthanum spin S) can be described in the laboratory frame (L) by the Hamiltonian [7,15]:

$$H_{DD}^{(L)}(I_i,P) = a_D^{I_iP}\sum_{m=-2}^{2}(-1)^m D_{0,m}^2(\Omega_{I_iP}^L)T_{2,-m}(I_i,P). \quad (1)$$

The particular components $T_{2,-m}(I_i, P)$ of the two-spin tensor operator have the form: $T_{2,0} = \frac{1}{\sqrt{6}}[2(I_i)_zP_z - \frac{1}{2}((I_i)_+P_- + (I_i)_-S_+)]$, $T_{2,\pm1} = \mp\frac{1}{2}[(I_i)_zP_\pm + (I_i)_\pm P_z]$, $T_{2,\pm2} = \frac{1}{2}(I_i)_\pm P_\pm$, while the dipole–dipole coupling constant is defined as: $a_D^{I_iP} = \sqrt{6}\frac{\mu_0}{4\pi}\frac{\gamma_I\gamma_P\hbar}{r_{I_iP}^3}$, where r_{I_iP} is the I_i–P inter-spin distance and the other symbols have their usual meaning. The Wigner rotation matrices $D_{0,m}^2(\Omega_{I_iP}^L)$ describe the orientation of the dipole–dipole axis for the pair of interacting spins with respect to the laboratory frame, encoded in the set of Euler angles $\Omega_{I_iP}^L$. The particular dipole–dipole interactions are modulated by jumps of the fluorine ions between equivalent (F_A–F_A, F_B–F_B) and non-equivalent (F_A–F_B) lattice sites. Important information on the dynamics of the fluorine ions in LaF_3 has been gained from the analysis of the fluorine lineshape [16,17], fluorine diffusion measurement by NMR gradient techniques [18] and some earlier relaxation studies performed at high magnetic field [14,19]. In [16,17] the two different fluorine subsystems have been clearly identified in the NMR spectrum by their chemical shifts. It has been observed that fast fluorine motion within the F_A sublattice leads to a narrowing of the corresponding resonance line, while the F_B line stays broad until it collapses with the faster one. It is worthwhile to mention that also other experimental techniques providing directly some macroscopic physical quantities, like fluorine conductivity [20,21] have been applied to investigate the fluorine dynamics.

Lanthanum spins exhibit within the LaF_3 crystal structure a static quadrupole coupling $H_Q^0(S)$, defined as the long-time averaged value of their quadrupole interaction, $H_Q^0(S) = \langle H_Q(S)(t)\rangle$. Since all crystallographic positions of lanthanum ions are equivalent, quadrupole couplings of individual spins, $H_Q(S_i)$, can be described by one Hamiltonian $H_Q(S)$. The averaged part of the lanthanum quadrupole interaction is determined in the laboratory frame (L) by the static quadrupole coupling constant a_Q^0, the asymmetry parameter η_0 and the orientation of the principal axis system of the electric field gradient tensor relative to the (L) frame, given by the angles Ω_Q^L [7,15]

$$H_Q^{0(L)} = \frac{1}{2}\sqrt{\frac{3}{2}}\frac{a_Q^0}{S(2S-1)}\sum_{m=-2}^{2}(-1)^m \times\left[D_{0,m}^2\left(\Omega_Q^L\right) + \frac{\eta_0}{\sqrt{6}}\left(D_{2,m}^2\left(\Omega_Q^L\right) + D_{-2,m}^2\left(\Omega_Q^L\right)\right)\right]T_{2,-m}(S). \quad (2)$$

The single-spin tensor operators $T_{2,-\mathrm{m}}(S)$ are now defined as: $T_{2,0}(S)=\frac{1}{\sqrt{6}}[3S_z^2-S(S+1)]$, $T_{2,\pm1}(S)=\mp\frac{1}{2}[S_zS_\pm+S_\pm S_z]$, $T_{2,\pm2}(S)=\frac{1}{2}S_\pm S_\pm$.

The mutual dipole–dipole coupling between the non-equivalent fluorine spins from the distinct sublattices F_A and F_B implies that the rate of change of the component of the F_A spins along the z axis $\langle I_z^A\rangle$ depends upon the component of the F_B spins $\langle I_z^B\rangle$ and vice versa. The relevant longitudinal magnetizations exhibit biexponential recoveries, and their evolution is governed by the set of equations [1,6,14]:

$$\frac{\mathrm{d}\langle I_z^A\rangle}{\mathrm{d}t}=a_{AA}\left(\langle I_z^A\rangle-\langle I_z^A\rangle_0\right)+a_{AB}\left(\langle I_z^B\rangle-\langle I_z^B\rangle_0\right), \tag{3a}$$

$$\frac{\mathrm{d}\langle I_z^B\rangle}{\mathrm{d}t}=a_{BA}\left(\langle I_z^A\rangle-\langle I_z^A\rangle_0\right)+a_{BB}\left(\langle I_z^B\rangle-\langle I_z^B\rangle_0\right). \tag{3b}$$

The coefficients a_{AA}, a_{BB}, a_{AB}, a_{BA} contain in addition to the specific dipolar relaxation rates, denoted respectively, as R_1^{AA}, R_1^{BB}, R_1^{AB}, R_1^{BA}, the exchange rates τ_{AB}^{-1}, τ_{BA}^{-1} between the non-equivalent lattice sites

$$a_{AA}=-R_1^{AA}-\frac{1}{\tau_{AB}},\quad a_{AB}=-\frac{N_A}{N_B}R_1^{AB}+\frac{1}{\tau_{BA}}. \tag{4}$$

The remaining coefficient a_{BB}, a_{BA} can be obtained from Eq. (4) by replacing the index A by B and vice versa. The exchange lifetime τ_{AB} is related to τ_{BA} by the ratio of the numbers of the fluorine spins in the subsystems F_A and F_B: $\tau_{AB}=\frac{N_A}{N_B}\tau_{BA}$. The relaxation rates R_1^{AA} (R_1^{BB}) contain terms corresponding to the three relaxation pathways of fluorine spins, created, respectively, by dipole–dipole couplings within one sublattice $R_{1(A\to A)}^{AA}(R_{1(B\to B)}^{BB})$, couplings between spins from different fluorine sublattices $R_{1(A\to B)}^{AA}(R_{1(B\to A)}^{BB})$ and fluorine–lanthanum dipolar interactions $R_{1(A\to La)}^{AA}(R_{1(B\to La)}^{BB})$:

$$R_1^{AA}=R_{1(A\to A)}^{AA}+R_{1(A\to B)}^{AA}+R_{1(A\to La)}^{AA}, \tag{5a}$$

$$R_1^{BB}=R_{1(B\to B)}^{BB}+R_{1(B\to A)}^{BB}+R_{1(B\to La)}^{BB}. \tag{5b}$$

The first two contributions are given by the well known expressions for the dipolar spin–lattice relaxation rates for like and unlike nuclei with the spins 1/2, respectively [1–4,6,7,14,15]:

$$R_{1(A\to A)}^{AA}=\left(\frac{\mu_0}{4\pi}\gamma_I^2\hbar\right)^2 I(I+1)\left[J_{AA}^{(1)}(\omega_A)+4J_{AA}^{(2)}(2\omega_A)\right], \tag{6a}$$

$$R_{1(A\to B)}^{AA}=\left(\frac{\mu_0}{4\pi}\gamma_I^2\hbar\right)^2 I(I+1)\frac{1}{3}\left[J_{AB}^{(0)}(\omega_A-\omega_B)+3J_{AB}^{(1)}(\omega_A)+6J_{AB}^{(2)}(\omega_A+\omega_B)\right]. \tag{6b}$$

The cross-relaxation rates R_1^{AB} (R_1^{BA}), linking the evolution of the magnetizations $\langle I_z^A\rangle$ and $\langle I_z^B\rangle$, have also the well-known forms [1,6,7,14,15]

$$R_1^{AB}=\left(\frac{\mu_0}{4\pi}\gamma_I^2\hbar\right)^2 I(I+1)\frac{1}{3}\left[-J_{AB}^{(0)}(\omega_A-\omega_B)+6J_{AB}^{(2)}(\omega_A+\omega_B)\right]. \tag{7}$$

Corresponding expressions for the relaxation rates R_1^{BB} and R_1^{BA} can be obtained by changing the indices $A\to B$ and $B\to A$ in Eqs. (6) and (7). The spectral densities are related to structural and motional parameters of the fluorine spins in the LaF_3 crystal lattice. We assume in this paper, following [14], that the dipole–dipole correlation function for the pair of fluorine spins I_i-I_j: $\left\langle\frac{D_{0,K}^{2*}(\Omega_{I_iI_j}^L(t))}{r_{I_iI_j}^3(t)}\frac{D_{0,K}^2(\Omega_{I_iI_j}^L(0))}{r_{I_iI_j}^3(0)}\right\rangle$ can be modeled as a single exponential decay. This assumption implies Lorentzian forms of the spectral densities occurring in Eqs. (6a,6b,7,14,15)

$$J_{\alpha\beta}^{(K)}(\omega)=\sum_j\left(\frac{D_{0,K}^2\left(\Omega_{I_iI_j}^L\right)}{r_{I_iI_j}^3}\right)^2\frac{2\tilde{\tau}_{\alpha\beta}}{1+\omega^2\tilde{\tau}_{\alpha\beta}^2};\quad \alpha,\beta=A,B;\quad I_i\neq I_j, \tag{8}$$

where the summation is performed over spins I_j from the sublattice β involved in the relaxation processes of the spin I_i from the α sublattice (α, $\beta=A$, B). The correlation time $\tilde{\tau}_{\alpha\beta}$ describes the fluctuation of the dipole–dipole coupling due to the motion of both coupled spins and therefore it is determined by the superposition of the two specific correlation rates $\tau_A^{-1},\tau_B^{-1}:\tilde{\tau}_{\alpha\beta}^{-1}=\tau_\alpha^{-1}+\tau_\beta^{-1}$, containing the effects of ion jumps within the particular sublattices (described by the time constants τ_{AA} and τ_{BB}) and between them (τ_{AB}, τ_{BA}): $\tau_A^{-1}=\tau_{AA}^{-1}+\tau_{AB}^{-1}$, $\tau_B^{-1}=\tau_{BB}^{-1}+\tau_{BA}^{-1}$.

To obtain a complete description of the fluorine spin relaxation one needs to specify the contributions from lanthanum spins: $R_{1(A\to La)}^{AA}$ and $R_{1(B\to La)}^{BB}$. Transitions of fluorine spins leading to their longitudinal relaxation are accompanied by lanthanum spin transitions between energy levels determined by a superposition of the static quadrupole interaction $H_Q^0(S)$ [Eq. (2)] and the lanthanum Zeeman coupling $H_Z(\bar{S})$. The 'classical' SBM approach to dipolar relaxation, developed under the assumption of a Zeeman energy structure for both interacting spins, cannot be treated as a proper description of fluorine spin relaxation caused by coupling to lanthanum spins, if the condition $H_Z(S)\gg H_Q^0(S)$ is not fulfilled (i.e., if the quadrupole effects on the energy level structure of the lanthanum spins are non-negligible).

We wish to point out clearly that we assume in this paper that the dipolar as well as the quadrupole spins obey the conditions of the Redfield theory [5–7]. Applying the perturbation treatment to an arbitrary spin system some caution must be exercised regarding its validity conditions. The Redfield theory has two essential limitations:

1. The perturbing Hamiltonian $H_1(t)$ (expressed in the angular frequency units) has to fulfill the condition: $|H_1\tau_c|\ll 1$, where τ_c is the correlation time for the perturbing interaction. This condition implies that the resulting relaxation timescale is much slower than the fluctuations causing the relaxation.

2. The main Hamiltonian H_0 must obey the relation $|H_0| \gg |H_1||H_1\tau_c|$, which guaranties that the oscillating factors $(\omega_{\alpha\alpha'} - \omega_{\beta\beta'})t$ associated with the particular relaxation rates $R_{\alpha\alpha'\beta\beta'}$ and resulting from the transformation to the interaction representation (generated by the main Hamiltonian) are effectively averaged out, unless they are equal zero.

If the conditions are not fulfilled one cannot define explicitly time-independent relaxation rates. Therefore, the perturbation approach, in particular the Solomon formulation, can be used to describe the fluorine relaxation processes, if the dipole–dipole interactions responsible for the relaxation fulfill the conditions $|H_{DD}(I_\alpha, I_\beta)\tilde{\tau}_{\alpha\beta}| < 1$ and $|H_{DD}(I_\alpha, S)\tilde{\tau}_{\alpha La}| < 1$. The strongest dipole–dipole interactions in LaF_3 are about 20 kHz. Thus, one can estimate that the perturbation theory can be applied if the relevant correlation times are shorter than 5×10^{-6} s. In fact the time scales of the fluorine motion within the individual sublattices, as well as between them depend strongly on the temperature and eventual admixtures (for example by Sr^{2+} ions, as we shall see later). The Redfield condition is relatively easy to fulfill for these relaxation channels, which involve the F_A fluorine spins. They jump diffusion between the equivalent lattice sites is the fastest dynamic process within the LaF_3 crystal lattice. According to the literature data [14,17] the correlation time τ_{AA} is of the order 10^{-5}–10^{-6} s at room temperature, and of the order 10^{-10} s at $T = 1000$ K [14], while the for the correlation time τ_{AB} it has been obtained 10^{-4} s at room temperature and 10^{-5}–10^{-6} s at 1000 K [14]. It indicates that for higher temperatures or crystals containing some admixtures the perturbation approach to the fluorine spins relaxation is appropriate. Nevertheless, for individual cases on should consider with caution the validity conditions formulated above.

3. Theory of spin–lattice relaxation of 1/2 spins induced by dipole–dipole couplings to quadrupole spins

We formulate in the next section a general description of frequency-dependent relaxation of a spin 1/2 through its dipolar coupling to an ensemble of quadrupole spins, in the framework of solid state dynamics, where jump diffusion is the main motional process. Our model includes dynamics of the quadrupole spins by a proper description of their multiexponential and also frequency-dependent relaxation. We prove that the general approach converges to the Solomon expression in the high field limit.

3.1. Field-dependent relaxation of spins 1/2 by dipolar couplings to quadrupole spins

Relaxation processes of a spin I caused by a mutual coupling to a spin S can be described in the framework of the Liouville formalism by the relaxation superoperator $\hat{R}_I$ defined as [22–27]

$$\hat{\hat{R}}_{1(I\to S)} = -\int_0^\infty \mathrm{Tr}_S\left\{\hat{\hat{L}}_{IS}\exp\left[-\mathrm{i}\left(\hat{\hat{L}}_I + \hat{\hat{L}}_S\right)t\right]\hat{\hat{L}}_{IS}|\rho_S^{\mathrm{eq}})\right\}\mathrm{d}t, \tag{9}$$

where $\hat{\hat{L}}_I$ and $\hat{\hat{L}}_S$ are Liouville operators for the spins I and S, respectively, whereas $\hat{\hat{L}}_{IS}$ is the interaction Liouvilian. In the considered case the operator $\hat{\hat{L}}_I$ is just generated by the Zeeman Hamiltonian of the spin I, while the dipole–dipole interaction provides the I–S coupling, represented by the operator $\hat{\hat{L}}_{IS}$. The operator $\hat{\hat{L}}_S$ covers the main interactions for the spin S (the static quadrupole coupling and the Zeeman interaction) as well as its relaxation dynamics. The equilibrium density operator of the spin S is denoted as ρ_S^{eq}. To evaluate the relaxation operator according to the above formulation it is necessary to isolate from the dipole–dipole Hamiltonian $H_{DD}^{(L)}$ of Eq. (1), the part associated only with the dipolar spin I. One can achieve this expressing the second order tensor operators $T_{2,-m}(I,S)$ in terms of the first order tensors I_n^1 and S_n^1 [8–12,29]:

$$H_{DD}^{(L)}(I,S) = a_D^{IS}\sqrt{30}\sum_{n=-1}^{1}(-1)^n I_{-n}^{1(L)} \times\left\{\sum_{q=-1}^{1}\begin{pmatrix}2 & 1 & 1\\ n-q & q & -n\end{pmatrix}S_q^{1(L)}D_{0,n-q}^2\left(\Omega_{IS}^L\right)\right\}, \tag{10}$$

where the tensor components are related to the angular momentum operators $P_0^1 = P_z, P_{\pm1}^1 = \frac{1}{\sqrt{2}}P_\pm, P = I, S$, and $\begin{pmatrix}2 & 1 & 1\\ n-q & q & -n\end{pmatrix}$ are the appropriate $3-j$ symbols. The indexes (L) in the operators $I_{-n}^{1(L)}$ and $S_q^{1(L)}$ indicate explicitly that we consider the representation of the dipole–dipole interaction in the laboratory frame. On the background of Eq. (9) one can express the spin–lattice relaxation of the spin $I = 1/2$ caused by the I–S dipole–dipole coupling as the real part of the complex dipolar spectral density K_{IS}^{DD} taken at the negative Larmor frequency of the spin I: $R_{1(I\to S)} = 2\mathrm{Re}\{K_{IS}^{DD}(-\omega_I)\}$ [8–12]. The spectral density results from Eq. (9) by inserting the interaction Liouville superoperator $\hat{\hat{L}}_{IS}$ (generated by the dipolar Hamiltonian of Eq. (10)) and the Liouvilian $\hat{\hat{L}}_I = [\omega_I I_Z, \ldots]$

$$K_{IS}^{DD}(-\omega_I) = 30\left(\frac{\mu_0\hbar\gamma_I\gamma_S}{4\pi}\right)^2\frac{1}{2S+1} \times\sum_{p,q}\begin{pmatrix}2 & 1 & 1\\ 1-q & q & -1\end{pmatrix}\begin{pmatrix}2 & 1 & 1\\ 1-p & p & -1\end{pmatrix} \times\int_0^\infty \mathrm{Tr}_S\left\{S_q^{1+(L)}\exp(-\mathrm{i}\hat{\hat{L}}_S t)S_p^{1(L)}\right\} \times\left\langle\frac{D_{0,1-q}^{2*}\left(\Omega_{IS}^L(t)\right)}{r_{IS}^3(t)}\frac{D_{0,1-p}^2\left(\Omega_{IS}^L(0)\right)}{r_{IS}^3(0)}\right\rangle\exp(-\mathrm{i}\omega_I t)\mathrm{d}t. \tag{11}$$

The factor $(2S+1)^{-1}$ originates from the equilibrium density operator ρ_S^{eq} in the high temperature approximation

[7–12]. Because of the limited space, the calculations are not presented here in great detail. More comments and explanations on the applied formalism are available as Supplementary material. We separate in the above formulation the correlation functions of the p–q components of the dipolar coupling strength, $c_{IS}^{qp}(t) = \langle \frac{D_{0,1-q}^{2*}(\Omega_{IS}^{L}(t))}{r_{IS}^{3}(t)} \frac{D_{0,1-p}^{2}(\Omega_{IS}^{L}(0))}{r_{IS}^{3}(0)} \rangle$, from the correlation functions, $\mathrm{Tr}_S\{S_q^{1+(L)} \exp(-\mathrm{i}\hat{\hat{L}}_S t) S_p^{1(L)}\}$, representing the S spin dynamics. The quantities $\frac{D_{0,1-p}^{2}(\Omega_{IS}^{L})}{r_{IS}^{3}}$ change in time due to motion of the spin I, which neither affects the energy level structure nor the relaxation processes of the spin S. Therefore, the dynamics of the S spin is completely independent of the spin I. We have assumed (setting up Eq. (8)) that the correlation function $c_{IS}^{qp}(t)$, determined for solid state systems mainly by the jump diffusion, is single exponential

$$\left\langle \frac{D_{0,1-q}^{2*}(\Omega_{IS}^{L}(t))}{r_{IS}^{3}} \frac{D_{0,1-p}^{2}(\Omega_{IS}^{L}(0))}{r_{IS}^{3}} \right\rangle = \frac{D_{0,1-q}^{2*}(\Omega_{IS}^{L})}{r_{IS}^{3}} \frac{D_{0,1-p}^{2}(\Omega_{IS}^{L})}{r_{IS}^{3}} \exp\left(-\frac{\tau}{\tilde{\tau}_{IS}}\right). \tag{12}$$

Thus, using the last step, one obtains for the spectral density $K_{IS}^{DD}(-\omega_I)$ the expression

$$K_{IS}^{DD}(-\omega_I) = 30\left(\frac{\mu_0 \hbar \gamma_I \gamma_S}{4\pi}\right)^2 \frac{1}{2S+1} \times \sum_{p,q} \begin{pmatrix} 2 & 1 & 1 \\ 1-q & q & -1 \end{pmatrix} \begin{pmatrix} 2 & 1 & 1 \\ 1-p & p & -1 \end{pmatrix} \times \frac{D_{0,1-q}^{2*}(\Omega_{IS}^{L})}{r_{IS}^{3}} \frac{D_{0,1-p}^{2}(\Omega_{IS}^{L})}{r_{IS}^{3}} \sigma_S^{qp}(-\omega_I), \tag{13}$$

where $\sigma_S^{qp}(-\omega_I)$ represents the quadrupole spin spectral density (including in addition to the S spin dynamics the modulation of the mutual I–S dipole–dipole coupling by the jump diffusion)

$$\sigma_S^{qp}(-\omega_I) = \int_0^\infty \mathrm{Tr}_S\left\{ S_q^{1+} \exp\left[-\left(\mathrm{i}\hat{\hat{L}}_S + \frac{1}{\tilde{\tau}_{IS}} + \mathrm{i}\omega_I \right) t \right] S_p^1 \right\} \mathrm{d}t. \tag{14}$$

To calculate the spectral densities $\sigma_S^{qp}(-\omega_I)$, we turn to the quadrupole spin dynamics and specify the Liouville operator $\hat{\hat{L}}_S$. For this purpose we have to discuss in more details the S spin relaxation.

We assume in this paper that the quadrupole spin fulfills the requirements of the Redfield relaxation theory [1–7]. It means that one can set up the equation of motion of the quadrupole spin density operator $\hat{\hat{\sigma}}_S(t)$ in the form

$$\frac{\partial}{\partial t}\left|\hat{\hat{\sigma}}_S(t)\right\rangle = -\hat{\hat{L}}_S\left|\hat{\hat{\sigma}}_S(t)\right\rangle = -\left(\hat{\hat{L}}_S^0 - \mathrm{i}\hat{\hat{R}}_S\right)\left|\hat{\hat{\sigma}}_S(t)\right\rangle. \tag{15}$$

The time-independent operator $\hat{\hat{L}}_S^0$ is generated by the main, unperturbed Hamiltonian $H_S^{0(L)}$ obtained as a combination of the Zeeman coupling $H_z^{(L)}(S) = \omega_S S_z$, where ω_S is the quadrupole spin Larmor frequency and the static quadrupole interaction $H_Q^{0(L)}$ of Eq. (2): $H_S^{0(L)} = H_z^{(L)}(S) + H_Q^0$. The index (L) indicates that we consider both interactions in the laboratory frame. The quadrupole spin is quantized along the principal axis of the main Hamiltonian $H_S^{0(L)}$ and the energy level structure is given by its eigenvalues. The second term in Eq. (15) contains the relaxation superoperator $\hat{\hat{R}}_S$. Most of the essential elements of the further considerations of this chapter have been presented in the series of papers [8–11], devoted to the problem of nuclear spin relaxation enhanced by electron spin dynamics (the PRE effects). However, for the sake of clarity and completeness of the current paper dealing with solid state dynamics and quadrupole spins, we provide some details of the evaluation of the quadrupole spin relaxation. The Redfield theory gives the quadrupole spin relaxation rates $R_{\alpha\alpha'\beta\beta'}^S$ in terms of the matrix elements of the relaxation superoperator $\hat{\hat{R}}_S$, connecting the evolution of the coherences $(\sigma_S)_{\alpha\alpha'}$ and $(\sigma_S)_{\beta\beta'}$ [6,7,22,23,27]

$$\frac{\mathrm{d}(\sigma_S)_{\alpha\alpha'}(t)}{\mathrm{d}t} = -\mathrm{i}\omega_{\alpha\alpha'}(\sigma_S)_{\alpha\alpha'}(t) + \sum_{\beta\beta'} R_{\alpha\alpha'\beta\beta'}^S \left((\sigma_S)_{\beta\beta'}(t) - \left(\sigma_{S'}^0\right)_{\beta\beta'} \right). \tag{16}$$

The appropriate Liouville basis $\{|\psi_\alpha^S\rangle\langle\psi_{\alpha'}^S|\}$ is generated by the set of eigenstates $\{|\psi_\alpha^S\rangle\}$ of the main Hamiltonian $H_S^{0(L)}$. The frequency $\omega_{\alpha\alpha'} = \omega_\alpha - \omega_{\alpha'}$ in Eq. (16) is the transition frequency between the two energy levels E_α and $E_{\alpha'}$ corresponding to the eigenstates $|\psi_\alpha^S\rangle$ and $|\psi_{\alpha'}^S\rangle$. The eigenstates $|\psi_\alpha^S\rangle$ can be expressed in terms of the Zeeman basis functions of the quadrupole spin, $|r\rangle = |S, m_S\rangle$ (S and m_S are, respectively, the spin- and magnetic-quantum numbers), by the relation: $|\psi_\alpha^S\rangle = \sum_{m_S=-S}^{S} c_{\alpha m_S} |S, m_S\rangle$, where the specific coefficients can be obtained by a diagonalization of the matrix representation of the Hamiltonian $H_S^{0(L)}$ in the Zeeman basis [9–11]. In the next step we aim at an explicit evaluation of the quadrupole spin relaxation rates $R_{\alpha\alpha'\beta\beta'}^S$. They are given as linear combinations of appropriate spectral densities taken at frequencies corresponding to differences between the energy levels [6,7,22,23,27,28]:

$$R_{\alpha\alpha'\beta\beta'}^S = J_{\alpha\beta\alpha'\beta}^S, (\omega_{\alpha\beta}) + J_{\alpha\beta\alpha'\beta}^S, (\omega_{\alpha'\beta'}) - \delta_{\alpha'\beta'} \times \sum_\gamma J_{\alpha\gamma\beta\gamma}^S(\omega_{\gamma\beta}) - \delta_{\alpha\beta} \sum_\gamma J_{\alpha'\gamma\beta'\gamma}^S(\omega_{\gamma\beta'}). \tag{17}$$

Here we consider the quadrupole relaxation mechanism provided by time fluctuations of the electric field gradient. The fluctuations create a perturbing, time-dependent Hamiltonian $H_Q^{T(L)}(t)$, defined as a deviation of the total quadrupole interaction $H_Q^{(L)}(t)$ from its average value: $H_Q^{T(L)}(t) = H_Q^{(L)}(t) - \langle H_Q^{(L)}(t)\rangle = H_Q^{(L)}(t) - H_Q^{0(L)}$. Thus, the spectral densities $J_{\alpha\alpha'\beta\beta}^S(\omega)$ are determined by the corresponding matrix elements of the perturbing Hamiltonian $H_Q^{T(L)}$ in the eigenbasis $\{|\psi_\alpha^S\rangle\}$ [6,7,22,23,27,28]

$$J^S_{\alpha\alpha'\beta\beta'}(\omega) = \int_0^\infty \left\langle \psi^S_\alpha \middle| H^{T(L)}_Q(0) \middle| \psi^S_{\alpha'} \right\rangle \left\langle \psi^S_\beta \middle| H^{T(L)}_Q(t) \middle| \psi^S_{\beta'} \right\rangle \times \exp(-\mathrm{i}\omega t)\,\mathrm{d}t. \quad (18)$$

Employing the relationship between the eigenvectors $|\psi^S_\alpha\rangle$ and the Zeeman functions $|r\rangle = |S,m_S\rangle$ one can represent the Hamiltonian matrix elements $\langle\psi^S_\alpha|H^{T(L)}_Q|\psi^S_{\alpha'}\rangle$ as: $\langle\psi^S_\alpha|H^{T(L)}_Q|\psi^S_{\alpha'}\rangle = \sum_{r,r'} c^*_{r\alpha} c_{r'\alpha'} \langle r|H^{T(L)}_Q|r'\rangle$. Therefore, the spectral densities $J^S_{\alpha\alpha'\beta\beta}(\omega)$ can be obtained explicitly from the formula

$$J^S_{\alpha\alpha'\beta\beta'}(\omega) = \sum_{r,r'} c^*_{r\alpha} c_{r'\alpha'} c^*_{r'\beta} c_{r\beta'} \int_0^\infty \left\langle r \middle| H^{T(L)}_Q(0) \middle| r' \right\rangle \times \left\langle r' \middle| H^{T(L)}_Q(t) \middle| r \right\rangle \exp(-\mathrm{i}\omega t)\,\mathrm{d}t. \quad (19)$$

Assuming the ordinary representation of the Hamiltonian $H^{T(L)}_Q(t)$ in terms of the tensor operators $T_{2,-m}(S)$ and corresponding spatial functions $A_m(t) : H^{T(L)}_Q(t) = \sum^2_{m=-2}(-1)^m T_{2,-m}(S) A_m(t)$ the spectral densities $J^S_{\alpha\alpha'\beta\beta}(\omega)$ can be related explicitly to the quantities $\tilde{J}^S_m(\omega) = \int_0^\infty \langle A^*_m(0) A_m(t)\rangle \exp(-\mathrm{i}\omega t)\,\mathrm{d}t$ by the expression:

$$\int_0^\infty \left\langle r \middle| H^{T(L)}_Q(0) \middle| r' \right\rangle \left\langle r' \middle| H^{T(L)}_Q(t) \middle| r \right\rangle \exp(-\mathrm{i}\omega t)\,\mathrm{d}t = \sum_{m=-2}^{2} |\langle r|T_{2,-m}|r'\rangle|^2 \tilde{J}^S_m(\omega). \quad (20)$$

Now, we can calculate explicitly the spectral densities σ^{pq}_S defined by Eq. (14). The matrix representation of the quadrupole spin operator $-\mathrm{i}\hat{\hat{L}}_S = -\mathrm{i}\hat{\hat{L}}^0_S + \hat{\hat{R}}_S$ in the Liouville basis set $|\psi^S_\alpha\rangle\langle\psi^S_{\alpha'}|$ (the operator $-\mathrm{i}\hat{\hat{L}}^0_S$ is represented by the transition frequencies $-\mathrm{i}\omega_{\alpha\alpha'}$, Eq. (16)) can be easily adapted for the total operator in Eq. (14) : $-\mathrm{i}\hat{\hat{L}}_S - (\frac{1}{\tilde{\tau}_{IS}} + \mathrm{i}\omega_I)\hat{\hat{1}}$, by including the diagonal terms: $\frac{1}{\tilde{\tau}_{IS}} + \mathrm{i}\omega_I$. The rank-one tensor operators for the quadrupole spin S^1_q can be also represented as matrices in the same Liouville basis. However, to achieve this we have to start from their representations in the basis constructed from the Zeeman eigenstates $|n\rangle = |S,m_S\rangle$ [9–11,29]:

$$S^1_0 = \sum_{m_S=-S}^{S} m_S |S,m_S\rangle\langle S,m_S,| \quad (21a)$$

$$S^1_1 = -\frac{1}{\sqrt{2}} \sum_{m_S=-S}^{S-1} \times \sqrt{(S-m_S)(S+m_S+1)}\,|S,m_S+1\rangle\langle S,m_S|, \quad (21b)$$

$$S^1_{-1} = \frac{1}{\sqrt{2}} \sum_{m_S=-S+1}^{S} \times \sqrt{(S+m_S)(S-m_S+1)}\,|S,m_S-1\rangle\langle S,m_S|. \quad (21c)$$

Using the above expansions of the tensor operators we evaluate their representations in the Liouville basis $|\psi_\alpha\rangle\langle\psi_{\alpha'}|$, from the inverse relation between the Zeeman states $|r\rangle = |S,m_s\rangle$ and the eigenstates of the Hamiltonian $H^{S(L)}_0 : |r\rangle = \sum_\alpha (c^{-1})_{r\alpha} |\psi^S_\alpha\rangle$. The set of coefficients $(c^{-1})_{r\alpha}$ can be obtained by inverting the matrix c (with the coefficients $c_{\alpha r}$) describing the Zeeman representation of the eigenstates $|\psi^S_\alpha\rangle$. Thus, the explicit, closed form of the quadrupole spectral densities σ^{qp}_S can be evaluated as, [9–12]:

$$\sigma^{qp}_S = \sum_{\mu\nu} [a^q]^*_\mu \left[\left(\mathrm{i}\hat{\hat{L}}^0_S + \mathrm{i}\omega_I \hat{\hat{1}} + \hat{\hat{R}}_S + \frac{1}{\tilde{\tau}_{IS}} \hat{\hat{1}} \right)^{-1} \right]_{\mu\nu} [a^p]_\nu, \quad (22)$$

where the summation goes over all the Liouville states $|\psi^S_\alpha\rangle\langle\psi^S_{\alpha'}|$. The vectors a^q (called projection vectors in [8–11]) contain the expansions coefficients of the tensor operators S^1_q in the Liouville basis. The coefficients for $S = 7/2$, appropriate for the lanthanum spins, are collected in Appendix of [11].

The final expression for the spin–lattice relaxation rate of a spin 1/2 due to a dipole–dipole coupling to a quadrupole spin S, obtained from Eq. (13) has the form (see Supplementary material)

$$R_{1(I\to S)} = \left(\frac{\mu_0 \hbar \gamma_I \gamma_S}{4\pi}\right)^2 S(S+1) \frac{2}{(2S+1)S(S+1)} \times \mathrm{Re}\left\{ \left|\frac{D^2_{0,0}}{r^3_{IS}}\right|^2 \sigma^{11}_S + 3\left|\frac{D^2_{0,1}}{r^3_{IS}}\right|^2 \sigma^{00}_S + 6\left|\frac{D^2_{0,2}}{r^3_{IS}}\right|^2 \sigma^{-1-1}_S + 2\sqrt{3}\frac{D^{2*}_{0,0} D^2_{0,1}}{r^6_{IS}} \sigma^{10}_S + 2\sqrt{6}\frac{D^{2*}_{0,0} D^2_{0,2}}{r^6_{IS}} \sigma^{1-1}_S + 6\sqrt{2}\frac{D^{2*}_{0,1} D^2_{0,2}}{r^6_{IS}} \sigma^{0-1}_S \right\}, \quad (23)$$

where it has been taken into account that $\sigma^{qp}_S = \sigma^{pq}_S$. In combination with the quadrupole spectral densities σ^{qp}_S [Eq. (22)] it provides a tool for interpretation of field-dependent relaxation studies on solid state systems containing dipolar and quadrupolar spins connected by mutual dipole–dipole couplings.

To complete the quite general considerations some more comments on the quadrupole spin spectral densities $\tilde{J}^S_m(\omega)$ [Eq. (20)] are appropriate. They must be evaluated according to a motional model. Physical mechanisms of the lattice dynamics causing modulations of the electric field gradient, which lead to the lanthanum spin relaxation, are a separate, complicate issue beyond the scope of the paper. However, one can express the lanthanum spin relaxation in terms of spectral densities containing only two parameters: an amplitude of the fluctuating part of the quadrupole Hamiltonian Δ_Q, and a time constant τ_Q reflecting the time scale of the fluctuations:

$$\tilde{J}^S_m(\omega) = \left[\frac{1}{2}\sqrt{\frac{3}{2}}\frac{\Delta_Q}{S(2S+1)}\right]^2 \frac{2}{5} \frac{\tau_Q}{1+\omega^2\tau^2_Q}. \quad (24)$$

This simplifies the description of the quadrupole relaxation as much as possible without losing its physical meaning. It is important to notice a flexibility of our model: a more

realistic description of the lattice dynamics relevant for the quadrupole interaction can be incorporated into the model in a straightforward manner by formulating a suitable expression for the spectral density $\tilde{J}_m^S(\omega)$.

Finishing this section we would like to comment on a very important aspect of the present approach. The essence of this treatment is the hierarchy of events: the dynamics of the quadrupole spin S is completely independent of the dipolar spin I, but on the contrary the degrees of freedom of the spin S influence strongly the relaxation processes of the spin I. This condition is obviously fulfilled if the spin S possesses an efficient relaxation pathway by its own. In the case of an electron spin $S \geqslant 1$ this predominated relaxation mechanism is provided by fluctuations of zero field splitting tensors [8–12] and it is in fact very efficient. The zero field splitting relaxation supposes to be replaced by the quadrupole interaction $H_Q^T(t)$ for quadrupole spin systems. However, in solid state phase relaxation processes of quadrupole spins caused by fluctuations of the electric field gradient tensor occur on a rather long time-scale. The quadrupole spin possesses also a second relaxation pathway via the dipole–dipole coupling to the spin I, fluctuating in time due to motion of the last one; actually in the case of LaF_3 due to the jump diffusion of the fluorine spins. If the second relaxation mechanism dominates over the quadrupole one, one cannot treat the quadrupole spin dynamics as independent of the presence of the dipolar spins. Nevertheless, if the quadrupole spin relaxation is slow (independently of its origin) compared to other sources of the modulations of the I–S dipole–dipole interaction, it can be neglected from the perspective of the spin I altogether and, in consequence one can describe the dipolar spin relaxation within the present theory.

In the next section, we discuss the limiting case of a dominating Zeeman interaction and a slow (relative to the jump diffusion motion) quadrupole relaxation and demonstrate that the general expression of Eq. (23) leads to the well known formula of Eq. (6b) (adjusted for the different quantum number of the S spin and its different gyromagnetic factor).

3.2. Limiting cases

If the dynamic processes encoded in the correlation time $\tilde{\tau}_{IS}$ are on a rapid time scale relative to the quadrupole relaxation, they provide the dominant contribution to the time fluctuations of the dipole–dipole coupling and the quadrupole relaxation in Eq. (22) may be omitted, as it has been discussed in the previous section. The off-diagonal elements of the Liouville supermatrix vanish in this case, while the diagonal part is given by the simplified operator $\mathrm{i}\hat{\hat{L}}_S^0 + \mathrm{i}\omega_I\hat{\hat{1}} + \frac{1}{\tilde{\tau}_{IS}}\hat{\hat{1}}$, with only one, field-independent correlation time $\tilde{\tau}_{IS}$. Thus, the resulting dipolar spin relaxation rate $R_{1(I\to S)}$ can be expressed as a sum of spectral densities of the form $\frac{2\tilde{\tau}_{IS}}{1+\omega^2\tilde{\tau}_{IS}^2}$, where the static quadrupole coupling affects the frequencies ω, containing besides the Larmor frequency ω_I of the spin I, the transition frequencies of the spin S between its energy levels. If the Zeeman coupling of the spin S dominates over the static quadrupole interaction, $|H_Z(S)| \gg |H_Q^0|$ the quadrupole spin exhibits obviously an energy level structure very close to the Zeeman one and the Zeeman states $|m_S\rangle$ form now the appropriate Liouville basis. Looking at the representation of the operators S_q^1 given by Eqs. (21a–c) one can easily conclude that the cross terms σ_S^{pq}, $p \neq q$ vanish. The remaining terms σ_S^{pp} take the form

$$\sigma_S^{pp} = \frac{1}{3}\frac{S(S+1)(2S+1)}{2}\frac{2\tilde{\tau}_{IS}}{1+(\omega_S^p+\omega_I)^2\tilde{\tau}_{IS}^2}, \tag{25}$$

where the spectral density σ_S^{00}, corresponding to the S_z operator, does not contain any transition frequency of the spin $S(\omega_S^0 = 0)$, while the terms σ_S^{11} and σ_S^{-1-1} generated by S_+ and S_- operators include the frequencies $-\omega_S$ and ω_S, respectively $(\omega_S^1 = -\omega_S,\ \omega_S^{-1} = \omega_S)$. Thus, in the high field limit and for slow relaxation processes of the quadrupole spin, the expression of Eq. (23) converges to the Solomon formulation:

$$R_{1(I\to S)} = \left(\frac{\mu_0}{4\pi}\gamma_I\gamma_S\hbar\right)^2 S(S+1) \times \frac{1}{3}\left[J_{IS}^{(0)}(\omega_I-\omega_S) + 3J_{IS}^{(1)}(\omega_I) + 6J_{IS}^{(2)}(\omega_I+\omega_S)\right] \tag{26a}$$

with the spectral densities $J_{IS}^{(K)}(\omega)$ defined by Eq. (8) and written now for the I–S pair of spins

$$J_{IS}^{(K)}\left(\omega_S^{1-K,1-K}+\omega_I\right) = \left(\frac{D_{0,K}^2(\Omega_{IS}^L)}{r_{IS}^3}\right)^2 \frac{2\tilde{\tau}_{IS}}{1+\left(\omega_S^{1-K,1-K}+\omega_I\right)^2\tilde{\tau}_{IS}^2}. \tag{26b}$$

Now we turn to the problem of field-dependent fluorine spin relaxation in the LaF_3 system and complete the description presented in Section 2.

4. Applications to the LaF_3 spin system

To get a complete description of the fluorine spin relaxation in the LaF_3 crystal lattice, valid for an arbitrary magnetic field, we need to specify the terms $R_{1(\alpha\to La)}^{\alpha\alpha}$ describing the relaxation of the fluorine spins from the sublattice $\alpha(\alpha = A, B)$ due to their coupling to the lanthanum spins. The relaxation rates $R_{1(\alpha\to La)}^{\alpha\alpha}$ can be obtained from Eq. (23) by replacing the quantities $\frac{D_{0,1-q}^{2*}(\Omega_{IS}^L)D_{0,1-p}^2(\Omega_{IS}^L)}{r_{IS}^6}$ (corresponding only to one spin S) by the appropriate lattice sums over the lanthanum spins S_i involved in the relaxation of the fluorine spin I_α : $\sum_i \frac{D_{0,1-q}^{2*}(\Omega_{I_\alpha S_i}^L)D_{0,1-p}^2(\Omega_{I_\alpha S_i}^L)}{r_{I_\alpha S_i}^6}$. Since the lanthanum ions are fixed in their sublattice, the correlation time $\tilde{\tau}_{IS}$ is determined only by the motion of the fluorine ions and is given by $\tilde{\tau}_{ALa}^{-1} = \tau_{AA}^{-1} + \tau_{AB}^{-1}$ and $\tilde{\tau}_{BLa}^{-1} = \tau_{BB}^{-1} + \tau_{BA}^{-1}$. Finally, one also has to set $\gamma_I = \gamma_F$, $\gamma_S = \gamma_{La}$, $\omega_S = \omega_{La}$ and $\omega_I = \omega_\alpha$.

The biexponential behavior of the fluorine magnetization becomes apparent by writing explicitly the solution of the set of equations, Eqs. (3a) and (3b)

$$R_{1I}^{\pm} = -\frac{1}{2}\left[(a_{AA}+a_{BB}) \pm \sqrt{(a_{AA}-a_{BB})^2 + 4a_{AB}a_{BA}}\right]. \quad (27)$$

The experimental data presented in the next section corresponds to the slower relaxation process.

Since we have experimental evidence that lanthanum spin relaxation is slow in the LaF_3 crystals (the lanthanum spin–lattice relaxation time measured at 8.5 T is of the order of tenths of ms) we neglect it altogether and focus our attention on the effects of the energy level structure of the quadrupole spins affecting the relaxation of the fluorine spins. We demonstrate in the next section that the quantization of the lanthanum spins is of primary importance for the dynamics of the dipolar fluorine spins.

5. Analysis of experimental results and discussion

We present examples of experimental relaxation profiles for fluorine spins in LaF_3 crystals, collected in the frequency range 2×10^4–4×10^7 Hz, and apply our model to understand the observed frequency dependencies.

The relaxation rates have been measured as a function of the magnetic field using the field cycling technique. This means, that the applied magnetic field has been switched during the experiment: the sample has been polarized in a high magnetic field and the measuring process, i.e., recording an FID following a 90° RF-pulse, took also place in a high magnetic field. Between these phases the field has been switched to a lower, adjustable value, in which the relaxation took place. Since the total fluorine magnetization has been monitored in the experiments, a biexponential decay according to Eq. (27) is expected. Nevertheless, only single exponential decays have been observed, which is due to the fact that the relative weight of the faster component is mostly negligible. Furthermore, the corresponding relaxation rates easily get too fast to be measured by the field-cycling technique due to the limited switching time of the magnetic field. As a consequence the measured fluorine relaxation rates correspond to the slower process, described by the quantity R_{1I}^{-} in Eq. (27).

The coefficients $a_{\alpha\alpha}$ contain the terms $R^{\alpha\alpha}_{1(\alpha\to La)}$ predicted by the general model of Eq. (23) with the appropriate lattice sums collected in Appendix A. The static quadrupole coupling of the lanthanum spins in the LaF_3 crystal lattice is set to $a_Q^0 = 15$ MHz, while the asymmetry parameter is $\eta_0 = 0.8$ [30]. The orientation of the electric field gradient tensor with respect to the laboratory frame is given by the angle $\Omega_Q^{(L)} = (0, 54^\circ, 0)$ [31]. We neglect the relaxation of lanthanum spins altogether, reducing the number of adjustable parameters. We only need to consider the diffusion of fluorine spins reflected by the three time constants: τ_{AA}, τ_{BB} and τ_{BA}. Since experimental fluorine NMR spectra show that the motion inside the sublattice F_B is relatively slow [14,17,32] only the two parameters, τ_{AA} and τ_{BA}, become relevant for our analysis. Since the time constants characterize different motional processes, they are uncorrelated. The same NMR spectra give us information about the chemical shift between the fluorine spins belonging to different sublattices: ≈170 ppm. The relevance of the $R^{\alpha\alpha}_{1(\alpha\to La)}$ relaxation channel compared to the fluorine ones $R^{\alpha\alpha}_{1(\alpha\to\alpha)}$ and $R^{\alpha\alpha}_{1(\alpha\to\beta)}$ is determined by the factor $\frac{\gamma_S^2 S(S+1)}{\gamma_I^2 I(I+1)}$ (which is equal to 0.47 in the case of the lanthanum S and fluorine I spins) scaled by the ratio of the corresponding lattice sums. In addition, one should take into account that the correlation times for the fluorine–lanthanum relaxation channels are longer than the correlation times associated with the corresponding fluorine–fluorine relaxation pathways, because in the first case only the fluorine spins are mobile (the lanthanum ions are fixed). In consequence, the efficiency of the fluorine spin relaxation due to the coupling to the lanthanum spins is comparable to the efficiency of the fluorine–fluorine relaxation.

In Figs. 2A and B fluorine relaxation profiles for a pure LaF_3 crystal collected at four temperatures: 700, 800 (Fig. 2A) and 750, 850 K (Fig. 2B) are shown. Together with the experimental results we present curves obtained by least-square fitting of the theoretical model with the two adjustable parameters τ_{AA} and τ_{BA}. We set $\tau_{BB} = 5\times10^{-5}$ s, however, this time constant even changed by an order of magnitude, does not influence significantly the theoretical curves. We have obtained for the particular temperatures—700 K:$\tau_{AA} = 2.8\times10^{-8}$ s, $\tau_{BA} = 3.1\times10^{-6}$ s; 750 K: $\tau_{AA} = 1.1\times10^{-8}$ s, $\tau_{BA} = 1.2\times10^{-6}$ s; 800 K: $\tau_{AA} = 6.3\times10^{-9}$ s, $\tau_{BA} = 2.6\times10^{-7}$ s; and 850 K: $\tau_{AA} = 5.2\times10^{-9}$ s, $\tau_{BA} = 1.2\times10^{-7}$ s.

To visualize the effect of the energy level structure of the lanthanum spins, determined for an arbitrary magnetic field by the static quadrupole interaction in combination with the Zeeman coupling, we plot in Figs. 2A and B corresponding theoretical curves for the same parameters but obtained from the Solomon formulation, Eq. (26a), for the terms $R^{\alpha\alpha}_{1(\alpha\to La)}$. The two descriptions agree in the high field limit, as discussed in Section 4. However, if the condition $H_Z(S) \gg H_Q^0(S)$ is not fulfilled the static quadrupole coupling of the lanthanum spins has a profound influence on the fluorine spin relaxation. Such effects have been discussed for static zero field splitting affecting electron spin energy levels and influencing in this way nuclear spin relaxation [8–12].

Frequency-dependent relaxation studies in ionic crystals (like LaF_3) are an attractive source of information about the ion dynamics causing high conductivity of ionic materials. Some interesting aspects of motional heterogeneity and dynamic models leading to non-exponential correlation functions [32] can be discussed on the background of relaxation experiments. To consider fine features of lattice dynamics for systems containing quadrupole spins one needs to describe properly the effects of the quadrupole spin quantization and its multiexponential, field-dependent relaxation (if there is no justification that the relaxation is

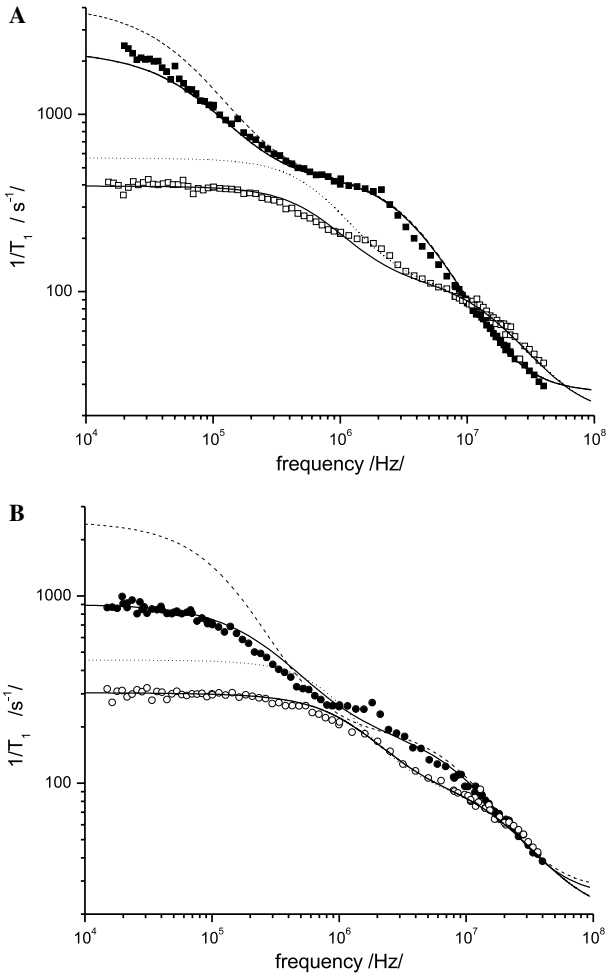

Fig. 2. Experimental fluorine spin relaxation rates for the pure LaF_3 crystal at the temperatures: (A) $T = 700$ K (solid squares) and $T = 800$ K (open squares), (B) $T = 750$ K (solid circles) and $T = 850$ K (open circles). Theoretical predictions of the present model obtained for $\tau_{AA} = 2.8 \times 10^{-8}$ s, $\tau_{BA} = 3.1 \times 10^{-6}$ s (700 K); $\tau_{AA} = 1.1 \times 10^{-8}$ s, $\tau_{BA} = 1.2 \times 10^{-6}$ s (750 K); $\tau_{AA} = 6.3 \times 10^{-9}$ s, $\tau_{BA} = 2.6 \times 10^{-7}$ s (800 K) and $\tau_{AA} = 5.2 \times 10^{-9}$ s, $\tau_{BA} = 1.2 \times 10^{-7}$ s (850 K) are presented as solid lines. Corresponding theoretical dependencies obtained from the Solomon formulation of the terms $R_{1(F_\alpha - La)}$, calculated for the same set of the parameters τ_{AA}, τ_{BA} are presented as the dashed (700, 750 K) and dotted (800, 850 K) lines.

negligible comparing to other sources of modulations of the mutual dipolar-spin-quadrupole–spin dipole–dipole coupling).

The discussed fluorine relaxation profiles (Figs. 2A and B) cannot be reproduced within the SBM formulation of the fluorine–lanthanum relaxation rates, $R^{\alpha\alpha}_{1(\alpha \to La)}$, by adjusting the correlation times τ_{AA} and τ_{BA}. To obtain an acceptable agreement with the experiments, one needs to allow a wide distribution of at least one of them. The same situation takes place in the case of fluorine relaxation in LaF_3 crystals doped slightly by Sr^{2+} ions. The doping influences the fluorine dynamics by introducing vacancies into the crystal lattice. In Figs. 3, 4A and B we present further examples of experimental fluorine relaxation profiles analyzed on the background of the present model. The profiles

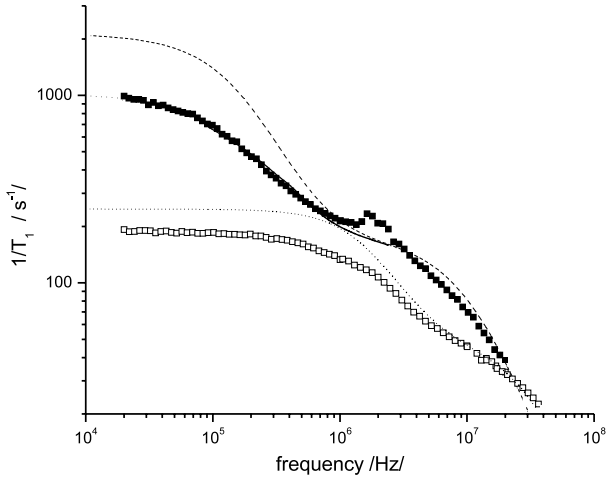

Fig. 3. Experimental fluorine spin relaxation rates for the LaF_3 crystal containing 0.01% Sr^{2+} admixtures collected at the temperatures $T = 700$ K (solid squares) and $T = 800$ K (open squares). Predictions of the present theoretical approach are shown as solid lines; $T = 700$ K; $\tau_{AA} = 1.1 \times 10^{-8}$ s, $\tau_{BA} = 1.1 \times 10^{-6}$ s; $T = 800$ K: $\tau_{AA} = 3.3 \times 10^{-9}$ s, $\tau_{BA} = 4.8 \times 10^{-7}$ s. Corresponding Solomon results are presented as the dashed (700 K) and dotted (800 K) lines.

in Fig. 3 are obtained for 0.01% concentration of Sr^{2+} ions in LaF_3 crystal lattice at the temperatures 700, 800 K and while Figs. 4A and B show fluorine relaxation data for LaF_3 crystal containing 0.3% Sr^{2+} ions, collected at the temperatures: 550 and 600 K. The correlation times τ_{AA} and τ_{BA} fitted to the experimental data are—700 K: $\tau_{AA} = 1.1 \times 10^{-8}$ s, $\tau_{BA} = 1.1 \times 10^{-6}$ s; 750 K: $\tau_{AA} = 4.9 \times 10^{-9}$ s, $\tau_{BA} = 5.3 \times 10^{-7}$ s; 800 K: $\tau_{AA} = 3.4 \times 10^{-9}$ s, $\tau_{BA} = 4.8 \times 10^{-7}$ s and 850 K: $\tau_{AA} = 2.5 \times 10^{-9}$ s, $\tau_{BA} = 2.5 \times 10^{-7}$ s for the material $LaF_3 + 0.01\%Sr^{2+}$; and 550 K: $\tau_{AA} = 9.5 \times 10^{-9}$ s, $\tau_{BA} = 3.1 \times 10^{-6}$ s; 600 K: $\tau_{AA} = 6.4 \times 10^{-9}$ s, $\tau_{BA} = 2.5 \times 10^{-6}$ s, for the material $LaF_3 + 0.3\%Sr^{2+}$.

Calculating the corresponding Solomon curves, we show that the proposed model and the traditional Solomon description predict at low field very different fluorine spin relaxation. To illustrate the statement, that one cannot obtain a satisfactory agreement with the experimental data on the background of the Solomon theory, we display also in Fig. 4B the result of analyzing the experimental data within the framework of the Solomon approach. The price one has to pay for the agreement at the low field, are significant discrepancies for higher magnetic fields. Therefore, even though the mean values of the τ_{AA} correlation time reported in [32] are comparable with the present results, the distribution of the correlation times assumed in [32] results from the oversimplified treatment of the fluorine–lanthanum relaxation pathway.

We wish to comment at the end, two features of the experimental fluorine relaxation data. We observe, especially in Figs. 4A and B that the fluorine relaxation profiles exhibit a plateau (or even a small maximum) at the frequencies $>10^7$ Hz. The relaxation rate does not decay to zero as expected. The investigated crystals contain unfortu-

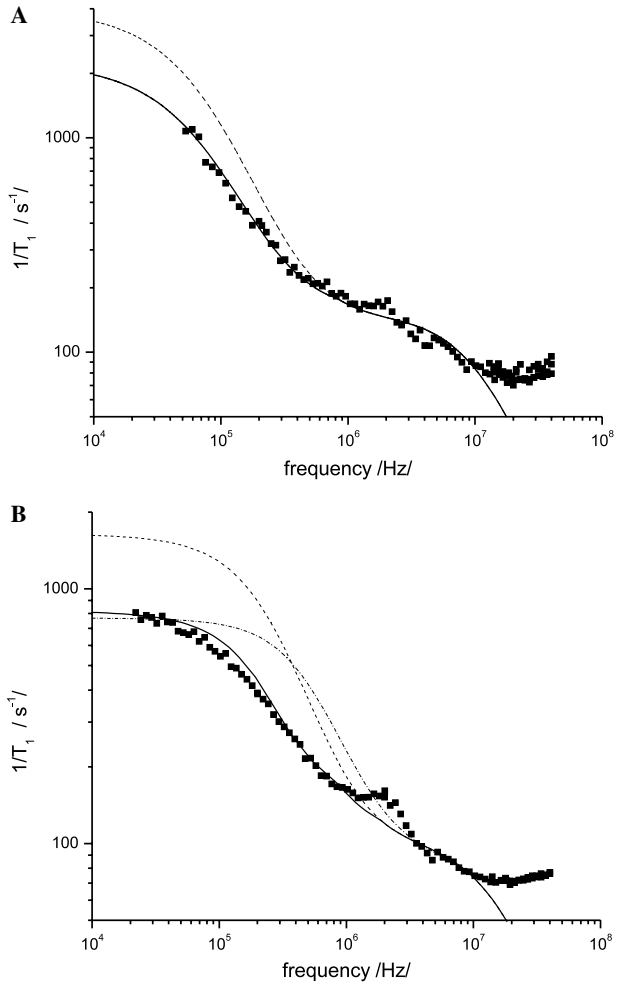

Fig. 4. Experimental fluorine spin relaxation rates for the LaF_3 crystal containing 0.3% Sr^{2+} admixtures collected at the temperatures: (A) $T = 550$ K and (B) $T = 600$ K. The solid lines show fluorine spin relaxation calculated on the background of the present model for $\tau_{AA} = 9.5 \times 10^{-9}$ s, $\tau_{BA} = 3.1 \times 10^{-6}$ s (550 K) and $\tau_{AA} = 6.4 \times 10^{-9}$ s, $\tau_{BA} = 2.5 \times 10^{-6}$ s (600 K), while corresponding predictions of the Solomon theory are presented as the dashed line. The dashed-dotted line in Fig. 4B represents calculations performed on the background of the SBM theory (applied to the terms $R_{1(F_A-La)}$) for the set of parameters: $\tau_{AA} = 5.4 \times 10^{-9}$ s, $\tau_{BA} = 2.8 \times 10^{-7}$ s, resulting in a good agreement with the experimental data at low field.

nately some paramagnetic impurities inducing an additional relaxation of neighboring fluorine spins. Taking into account typical profiles of paramagnetically induced nuclear spin relaxation, being constant in a wide frequency range and finally, after an eventual maximum decaying to zero, one could estimate this contribution and emulate it by adding a constant; for example ca. $20\ s^{-1}$ for the relaxation profile presented in Fig. 4B. We decided to neglect this effect altogether.

The second effect, we wish to comment is well visible in most of the presented cases in the frequency range 10^6–5×10^6 kHz and requires more attention. The relaxation profiles exhibit local maxima, caused by polarization transfer effects between fluorine and lanthanum spins. Fluorine polarization can be taken over, under certain conditions, by lanthanum spins. In the experiment, this effect is detected as a faster decay of the fluorine magnetization and interpreted as a local increasing (maximum) of the fluorine relaxation rate. The fluorine polarization can be transferred to lanthanum when the transition energy of fluorine spins (determined by their Zeeman interaction) is equal to some transition energies of lanthanum spins (determined by the lanthanum Zeeman- and quadrupole interactions) and if there is an efficient static I–S dipole–dipole coupling. The requirement that the mutual dipole–dipole interaction must be sensed by the participating spins as time independent means that the motional modulations of the relevant dipole–dipole coupling must be significantly slower than the fluorine spin relaxation. The F_B–La dipole–dipole coupling fluctuates in time slower than the F_A–La one, and is mainly modulated by the inter-lattice exchange, τ_{BA}. We tried to reproduce the relaxation profiles assuming the exchange lifetime τ_{BA} long enough to exclude the F_B–La dipole–dipole coupling as a relaxation pathway ($|H^{DD}_{B\to La}\tau_{BA}| \gg 1$) and treat it as the polarization transfer channel. It turned out that one cannot reproduce the fluorine relaxation profiles slowing down the exchange process. In addition, the time-scale of the exchange effects obtained from the already presented least-square fit has another experimental confirmation; it can be also deduced from fluorine line-shapes. Therefore, the observed polarization transfer effects suggest the presence of a relatively small fraction of weak-mobile fluorine ions, so that their dipolar interactions with lanthanum could cause the polarization transfer without significant effects on the relaxation picture.

6. Conclusions

We have developed a general model of field-dependent relaxation processes in solid state systems containing dipolar as well as quadrupole spins with mutual dipole–dipole couplings, valid for an arbitrary magnetic field. We have discussed in detail effects of the quadrupole spins energy level structure and their multiexponential relaxation on relaxation processes of the dipolar spins comparing the present description with the classical Solomon–Bloembergen–Morgan approach. Analogies between systems containing nuclear spins 1/2 coupled to electron spins and nuclear spins 1/2 coupled to quadrupole spins have been pointed out to give a better and more general understanding of dipolar relaxation processes in the presence of neighboring high spins.

The present approach has been applied to analyze fluorine spin–lattice relaxation processes in LaF_3 crystals containing two distinct fluorine sublattices. Comparisons with the Solomon predictions have been reported to show the necessity of an advanced theoretical treatment.

We believe that the theory presented in this paper, together with the illustrative calculations performed for the LaF_3 system can be useful for interpreting and understanding of field-dependent relaxation studies for variety of systems containing quadrupole spins.

Appendix A

The lattice sums $S^m_{F_\alpha \to F_\beta}$, $\alpha = 1,2,3$, $m = 0,1,2$ are defined as $S^m_{F_\alpha \to F_\beta} = \sum_i \frac{(D^2_{0,m}(\Omega^L_{I_\alpha (I_\beta)_i}))^2}{r^6_{I_\alpha (I_\beta)_i}}$. The summation is performed over fluorine spins $(I_\beta)_i$ belonging to the sublattice β and involved in relaxation processes of the fluorine spin I_α from the sublattice α. They are expressed in m^{-6} and listed below:

$$S^0_{F_1 \to F_1} = 4.08 \times 10^{57}, \quad S^1_{F_1 \to F_1} = 2.67 \times 10^{57}, \quad S^2_{F_1 \to F_1} = 2.7 \times 10^{57}$$

$$S^0_{F_2 \to F_2} = 9.56 \times 10^{56}, \quad S^1_{F_2 \to F_2} = 1.48 \times 10^{56}, \quad S^2_{F_2 \to F_2} = 2.56 \times 10^{56}$$

$$S^0_{F_3 \to F_3} = 8.41 \times 10^{56}, \quad S^1_{F_3 \to F_3} = 1.74 \times 10^{56}5, \quad S^2_{F_3 \to F_3} = 3.1 \times 10^{55}$$

$$S^0_{F_1 \to F_2} = 5.69 \times 10^{56}, \quad S^1_{F_1 \to F_2} = 2.03 \times 10^{57}, \quad S^2_{F_1 \to F_2} = 1.37 \times 10^{57}$$

$$S^0_{F_2 \to F_1} = 1.71 \times 10^{57}, \quad S^1_{F_2 \to F_1} = 6.09 \times 10^{57}, \quad S^2_{F_2 \to F_1} = 4.12 \times 10^{57}$$

$$S^0_{F_1 \to F_3} = 1.80 \times 10^{56}, \quad S^1_{F_1 \to F_3} = 8.23 \times 10^{56}, \quad S^2_{F_1 \to F_3} = 6.64 \times 10^{56}$$

$$S^0_{F_3 \to F_1} = 1.08 \times 10^{57}, \quad S^1_{F_3 \to F_1} = 4.94 \times 10^{57}, \quad S^2_{F_3 \to F_1} = 3.98 \times 10^{57}$$

$$S^0_{F_2 \to F_3} = 1.51 \times 10^{56}, \quad S^1_{F_2 \to F_3} = 1.01 \times 10^{56}, \quad S^2_{F_2 \to F_3} = 2.48 \times 10^{56}$$

$$S^0_{F_3 \to F_2} = 3.03 \times 10^{56}, \quad S^1_{F_3 \to F_2} = 2.01 \times 10^{56}, \quad S^2_{F_3 \to F_2} = 4.95 \times 10^{56}$$

The lattice sums $S^m_{F_\alpha \to La} = \sum_i \frac{(D^2_{0,m}(\Omega^L_{I_\alpha S_i}))^2}{r^6_{I_\alpha S_i}}$ are obtained by adding the contribution from the lanthanum spins S_i, relevant for relaxation of the fluorine spin I_α from the sublattice α.

$$S^0_{F_1 \to La} = 4.71 \times 10^{57}, \quad S^1_{F_1 \to La} = 2.6 \times 10^{57}, \quad S^2_{F_1 \to La} = 2.17 \times 10^{57}$$

$$S^0_{F_2 \to La} = 3.36 \times 10^{57}, \quad S^1_{F_2 \to La} = 1.23 \times 10^{57}, \quad S^2_{F_2 \to La} = 5.45 \times 10^{57}$$

$$S^0_{F_3 \to La} = 3.91 \times 10^{57}, \quad S^1_{F_3 \to La} = 3.56 \times 10^{56}, \quad S^2_{F_3 \to La} = 5.53 \times 10^{57}$$

Supplementary data

Supplementary data associated with this article can be found, in the online version, at doi:10.1016/j.jmr.2005.12.009.

References

[1] I. Solomon, Relaxation processes in a system of two spins, Phys. Rev. 99 (1955) 559–565.
[2] N. Bloembergen, L.O. Morgan, Proton relaxation times in paramagnetic solutions: effects of electron spin relaxation, J. Chem. Phys. 34 (1961) 842–850.
[3] R.E. Connick, D. Fiat, Oxygen-17 nuclear magnetic resonance study of the hydration shell of nickelous ion, J. Chem. Phys. 44 (1966) 4103–4107.
[4] J. Reuben, G.H. Reed, M. Cohn, NMR study of single-crystal glycine, J. Chem. Phys. 52 (1970) 1617.
[5] A.G. Redfield, The theory of relaxation processes, Adv. Magn. Reson. 1 (1965) 1–32.
[6] A. Abragam, The Principles of Nuclear Magnetism, Oxford University Press, Oxford, 1961.
[7] C.P. Slichter, Principles of Magnetic Resonance, Springer, Berlin, 1990.
[8] D. Kruk, J. Kowalewski, Nuclear spin relaxation in solution of paramagnetic systems ($S \geqslant 1$) under fast rotation conditions, J. Magn. Reson. 162 (2003) 229–240.
[9] I. Bertini, J. Kowalewski, T. Nilsson, G. Parigi, Nuclear spin relaxation in paramagnetic systems of $S = 1$: electron spin relaxation effects, J. Chem. Phys. 111 (13) (1999) 5795–5807.
[10] T. Nilsson, J. Kowalewski, Low field theory of nuclear spin relaxation in paramagnetic low-symmetry complexes for electron spin systems of $S = 1$, 3/2, 2, 5/2, 3 and 7/2, Mol. Phys. 98 (2000) 1617–1638, Erratum: Mol. Phys. 99 (2001) 369.
[11] D. Kruk, T. Nilsson, J. Kowalewski, Nuclear spin relaxation in paramagnetic systems with zero-field splitting and arbitrary electron spin, Phys. Chem. Chem. Phys. 3 (2001) 4907–4917.
[12] J. Kowalewski, D. Kruk, G. Parigi, NMR relaxation in solution of paramagnetic complexes: recent theoretical progress for $S \geqslant 1$, Adv. Inorg. Chem. 57 (2005) 41–104.
[13] B. Maximov, H. Schulz, Space group, crystal structure and twinning of lanthanum trifluoride, Acta Cryst. B 41 (1985) 88–91.
[14] G.A. Jaroszkiewicz, J.H. Strange, Motion on inequivalent lattice sites—NMR theory and application to LaF_3, J. Phys. C: Solid State Phys. 18 (1985) 2331–2349.
[15] R. Kimmich, NMR—Tomography, Diffusometry, Relaxometry, Springer, Berlin, Heildelberg, 1997.
[16] A.F. Privalov, H.-M. Vieth, I.V. Murin, Ionic motion in the LaF_3 superionic conductor studied by ^{19}F NMR with homonuclear decoupling, J. Phys. Chem. Solids 50 (1989) 395–398.
[17] A.F. Privalov, H.-M. Vieth, I.V. Murin, Nuclear magnetic resonance study of superionic conductors with tysonite structure, J. Phys.: Condens. Matter 6 (1994) 8237–8243.
[18] V.V. Sinitsyn, O. Lips, A.F. Privalov, F. Fujara, I.V. Murin, Transport properties of LaF_3 fast ionic conductor studied by field gradient NMR and impedance spectroscopy, J. Phys. Chem. Solids 64 (2003) 1201–1205.
[19] A.F. Aalders, A.F.M. Arts, H.V. de Wijn, Vacancy distribution and ionic motion in LaF_3 studied by ^{19}F NMR, Phys. Rev. B 32 (1985) 5412–5423.
[20] A. Roos, F.C.M. van de Pol, R. Keim, J. Schoonman, Ionic conductivity in tysonite-type solid solutions $La_{1-x}Ba_{x\ 3-x}$, Solid State Ionics 13 (1984) 191–203.
[21] H. Geiger, G. Schön, H. Stork, Ionic conductivity of single crystals of the non-stoichiometric tysonite phase $La_{(1-x)}Sr_xF_{(3-x)}$ ($0 \leqslant x \leqslant 0.14$), Solid State Ionics 15 (1985) 155–158.
[22] U. Fano, Description of states in quantum mechanics by density matrix and operator techniques, Rev. Mod. Phys. 29 (1957) 74–93.
[23] K. Blum, Density Matrix Theory and Applications, Plenum Press, New York, 1989.

[24] L.T. Muus, P.W. Atkins (Eds.), Electron Spin Relaxation in Liquids, Plenum Press, New York, 1972.
[25] C.N. Banvell, H. Primas, On the analysis of high-resolution nuclear magnetic resonance spectra: I. Methods of calculating NMR spectra, Mol. Phys. 6 (1963) 225–256.
[26] J. Jeener, Superoperators in magnetic resonance, Adv. Magn. Reson. 10 (1982) 1–51.
[27] R.R. Ernst, G. Bodenhausen, A. Wokaun, Principles of Nuclear Magnetic Resonance in One and Two Dimensions, Clarendom Press, Oxford, 1994.
[28] R.K. Wangsness, F. Bloch, The dynamic theory of nuclear induction, Phys. Rev. 89 (1953) 728–739.
[29] D.A. Varshalovich, A.N. Moskalev, V.K. Khersonskii, Quantum Theory of Angular Momentum, Word Scientific Publishing, Singapore, 1988.
[30] K. Lee, A. Sher, L.O. Andersson, W.G. Proctor, Temperature variation of La^{139} nuclear quadrupole resonance in LaF_3, Phys. Rev. 150 (1) (1966) 168–174.
[31] M. Matsushita, A. Mutoh, T. Kato, Coherent Raman spectroscopy of nuclear quadrupole resonance of La around Pr^{3+} in LaF_3, Phys. Rev. B 58 (21) (1998) 14372–14382.
[32] A.F. Privalov, O. Lips, F. Fujara, Dynamic processes in the superionic conductor LaF_3 at high temperatures as studied by spin–lattice relaxation dispersion, J. Phys.: Condens. Matter 14 (2002) 4515–4525.